J|A|C|S
ARTICLES
Published on Web 01/20/2007

Intermolecular Covalent $\pi-\pi$ Bonding Interaction Indicated by Bond Distances, Energy Bands, and Magnetism in Biphenalenyl Biradicaloid Molecular Crystal

Jingsong Huang* and Miklos Kertesz*

Contribution from the Department of Chemistry, Georgetown University, 37th & O Street, Washington, D.C. 20057-1227

Received September 5, 2006; E-mail: huangj2@georgetown.edu; kertesz@georgetown.edu

Abstract: Density-functional theory (DFT) calculations were performed for energy band structure and geometry optimizations on the stepped π-chain, the isolated molecule and (di)cations of the chain, and various related molecules of a neutral biphenalenyl biradicaloid (BPBR) organic semiconductor **2**. The dependence of the geometries on crystal packing provides indirect evidence for the intermolecular covalent $\pi-\pi$ bonding interaction through space between neighboring π-stacked phenalenyl units along the chain. The two phenalenyl electrons on each molecule, occupying the singly occupied molecular orbitals (SOMOs), are participating in the intermolecular covalent $\pi-\pi$ bonding making them partially localized on the phenalenyl units and less available for intramolecular delocalization. The band structure shows a relatively large bandwidth and small band gap indicative of good $\pi-\pi$ overlap and delocalization between neighboring π-stacked phenalenyl units. A new interpretation is presented for the magnetism of the stepped π-chain of **2** using an alternating Heisenberg chain model, which is consistent with DFT total energy calculations for **2** and prevails against the previous interpretation using a Bleaney−Bowers dimer model. The obtained transfer integrals and the magnetic exchange parameters fit well into the framework of a Hubbard model. All presented analyses on molecular geometries, energy bands, and magnetism provide a coherent picture for **2** pointing toward an alternating chain with significant intermolecular through-space covalent $\pi-\pi$ bonding interactions in the molecular crystal. Surprisingly, both the intermolecular transfer integrals and exchange parameters are larger than the intramolecular through-bond values indicating the effectiveness of the intermolecular overlap of the phenalenyl SOMO electrons.

Introduction

Phenalenyl is a well-known stable organic radical,[1] with its unpaired electron in the singly occupied molecular orbital (SOMO) (Chart 1). The phenalenyl radical and its derivatives have attracted much attention recently as a result of their very intriguing properties as shown, for example, in unusual multicenter covalent $\pi-\pi$ bonding[2−4] and in a wide range of electrical, optical, and magnetic properties.[5−7] A packing motif of π-dimerization has been observed in the solid state for the sterically crowded 2,5,8-tri-*tert*-butyl substituted phenalenyl radical (**1**) (Scheme 1).[8] ESR, UV−vis, and MS also confirm the π-dimerization of **1** in solutions[2] and even in the gas phase.[9] The intermolecular multicenter $\pi-\pi$ overlap due to the six pairs of spin-bearing carbon atoms (see the SOMO in Chart 1) and consequent pairing of the two SOMO electrons are the driving force for this π-dimerization, bringing two radicals of **1** slightly closer together (with an interplanar separation of 3.2−3.3 Å) than the sum of the van der Waals radii.[8] The interpretation of such short distances between radicals (neutral or charged) across $\pi-\pi$ overlaps has been in the focus of much recent research. This type of efficient intermolecular $\pi-\pi$ interaction has been recognized as a new class of multicenter covalent $\pi-\pi$

Chart 1. Phenalenyl Radical and Its SOMO

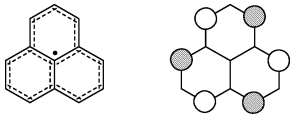

(1) (a) Reid, D. H. *Chem. Ind.* **1956**, 1504. (b) Gerson, F. *Helv. Chim. Acta* **1966**, *49*, 1463. For recent applications, see (c) Zheng, S.; Lan, J.; Khan, S. I.; Rubin, Y. *J. Am. Chem. Soc.* **2003**, *125*, 5786.
(2) Small, D.; Zaitsev, V.; Jung, Y.; Rosokha, S. V.; Head-Gordon, M.; Kochi, J. K. *J. Am. Chem. Soc.* **2004**, *126*, 13850.
(3) Takano, Y.; Taniguchi, T.; Isobe, H.; Kubo, T.; Morita, Y.; Yamamoto, K.; Nakasuji, K.; Takui, T.; Yamaguchi, K. *J. Am. Chem. Soc.* **2002**, *124*, 11122.
(4) Huang, J.; Kertesz, M. *J. Am. Chem. Soc.* **2006**, *128*, 7277.
(5) Pal, S. K.; Itkis, M. E.; Tham, F. S.; Reed, R. W.; Oakley, R. T.; Haddon, R. C. *Science* **2005**, *309*, 281.
(6) (a) Itkis, M. E.; Chi, X.; Cordes, A. W.; Haddon, R. C. *Science* **2002**, *296*, 1443. (b) Miller, J. S. *Angew. Chem., Int. Ed.* **2003**, *42*, 27.
(7) (a) Chi, X.; Itkis, M. E.; Patrick, B. O.; Barclay, T. M.; Reed, R. W.; Oakley, R. T.; Cordes, A. W.; Haddon, R. C. *J. Am. Chem. Soc.* **1999**, *121*, 10395. (b) Chi, X.; Itkis, M. E.; Kirschbaum, K.; Pinkerton, A. A.; Oakley, R. T.; Cordes, A. W.; Haddon, R. C. *J. Am. Chem. Soc.* **2001**, *123*, 4041. (c) Chi, X.; Tham, F. S.; Cordes, A. W.; Itkis, M. E.; Haddon, R. C. *Synth. Met.* **2003**, *133*, 367. (d) Pal, S. K.; Itkis, M. E.; Reed, R. W.; Oakley, R. T.; Cordes, A. W.; Tham, F. S.; Siegrist, T.; Haddon, R. C. *J. Am. Chem. Soc.* **2004**, *126*, 1478.
(8) (a) Goto, K.; Kubo, T.; Yamamoto, K.; Nakasuji, K.; Sato, K.; Shiomi, D.; Takui, T.; Kubota, M.; Kobayashi, T.; Takusi, K.; Ouyang, J. *J. Am. Chem. Soc.* **1999**, *121*, 1619. (b) Fukui, K.; Sato, K.; Shiomi, D.; Takui, T.; Itoh, K.; Gotoh, K.; Kubo, T.; Yamamoto, K.; Nakasuji, K.; Naito, A. *Synth. Met.* **1999**, *103*, 2257.
(9) Suzuki, S.; Morita, Y.; Fukui, K.; Sato, K.; Shiomi, D.; Takui, T.; Nakasuji, K. *J. Am. Chem. Soc.* **2006**, *128*, 2530.

10.1021/ja066426g CCC: $37.00

Scheme 1. π-Dimerization of 2,5,8-Tri-*tert*-butylphenalenyl Radical (**1**)

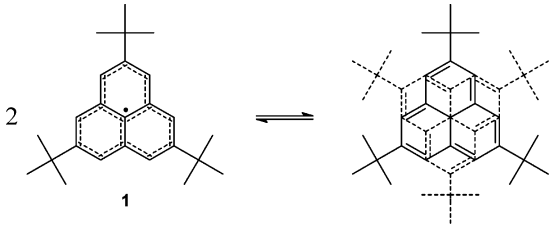

Scheme 2. Resonance Structures of Two Biphenalenyl Biradicaloid (BPBR) Molecules: 6,14-Diphenyl-*s*-indaceno-[1,2,3-*cd*:5,6,7-*c′d′*]diphenalene (**2**) and 4,8,12,16-Tetra-*tert*-butyl-*s*-indaceno[1,2,3-*cd*:5,6,7-*c′d′*]diphenalene (**3**)

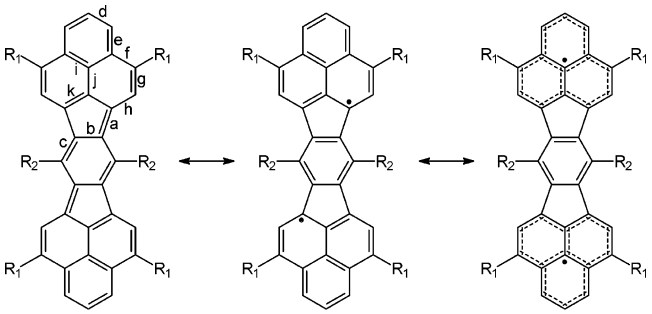

bonding,[2−4,10] leading to electron delocalization for both the classical charge transfer organic conductors,[11] and the more novel neutral radical organic conductors, such as the spiro-biphenalenyl (SBP) neutral radicals.[5−7,12]

In a recent paper, Kubo et al. reported a very interesting phenalenyl-based organic semiconductor with the building block of biphenalenyl biradicaloid (BPBR) molecule **2** (Scheme 2).[13] Scheme 2 also shows a similar molecule **3** with *tert*-butyl substitution.[14,15] Each BPBR consists of a central *s*-indacene-like moiety and two coplanar condensed phenalenyl units. As in **1**, each of these phenalenyl units contributes a SOMO. These SOMOs are perturbed in the BPBR compounds **2** and **3** owing to the *s*-indacene linkage as pointed out by Kubo et al.[13] Nevertheless, a key aspect of the properties of this family of compounds is based on the SOMO and the SOMO electrons. Both **2** and **3** have also resonance contributions coming from **2′**, **2″**, **3′**, and **3″**, which have more pronounced biradicaloid character as reflected by the localization of the SOMO electrons on the two phenalenyl units.

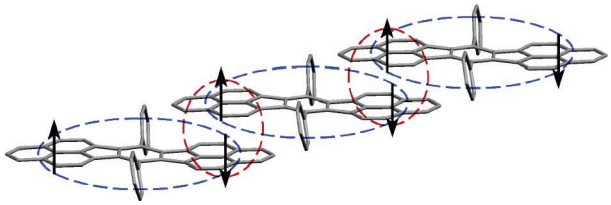

Figure 1. A stepped one-dimensional π-chain of molecules **2** excised from the crystal structure with interplanar separation of $D = 3.137$ Å.[13] The antiferromagnetic coupling is illustrated by ellipses (intra- and intermolecular couplings are indicated by horizontally and vertically oriented ellipses, respectively).

While **3** packs as an ordinary molecular crystal in which neighboring molecules of **3** are isolated from each other,[14,16] in contrast, **2** forms stepped quasi-one-dimensional (1-D) π-chains (Figure 1) in which the phenalenyl units display excellent step-to-step $\pi-\pi$ overlap between all six pairs of spin-bearing C atoms on π-stacked phenalenyls. The arrows indicate schematically the spins of the SOMO electrons in the phenalenyl units. The presence of significant *intra*molecular antiferromagnetic coupling in the molecular crystal of **3** between the two spins mediated by the *s*-indacene linkage has been established by Ohashi et al. using structural and spectroscopic characterizations.[14] By analogy to **3**, the intramolecular interaction between the two SOMO electrons in **2** should also persist with only small modification. The key question we raise is whether there exists an *inter*molecular antiferromagnetic coupling of two spins between π-stacked phenalenyl units along the chains of **2** and what are the effects on the physical properties of **2**.

The interplanar separation at $D = 3.137$ Å in the stepped chains of **2** is much shorter than the typical van der Waals distance indicating further attractive intermolecular interactions in addition to van der Waals forces. The through-space coupling of the two SOMO electrons across the $\pi-\pi$ overlap in the chain of **2** is therefore similar to the $\pi-\pi$ bonding present in the π-dimer of **1**, and it is reasonable to illustrate each of the SOMO electrons in the chain as being coupled intramolecularly to the other spin on the same molecule and intermolecularly to a third spin on a neighboring molecule (Figure 1). The effective $\pi-\pi$ overlap between the six pairs of spin-bearing C atoms of π-stacked phenalenyl units on neighboring molecules also leads to a large transfer integral, t,[17] or wide band dispersions along the chain direction.[13] Kubo et al. have seen indications of "strong intermolecular covalent character" in **2** on the basis of a dimer calculation; however, the covalent $\pi-\pi$ bonding interaction was described to play a role only in the resonance between intramolecular (Kekulé) and intermolecular interaction (biradical) as shown in Scheme 4 of ref 13 in contrast to our description of an alternating chain[18] shown in Figure 1. Accordingly, the SQUID-measured magnetic susceptibility of **2** was interpreted

(10) (a) Lü, J.-M.; Rosokha, S. V.; Kochi, J. K. *J. Am. Chem. Soc.* **2003**, *125*, 12161. (b) Novoa, J. J.; Lafuente, P.; Del Sesto, R. E.; Miller, J. S. *Angew. Chem., Int. Ed.* **2001**, *40*, 2540. (c) Del Sesto, R. E.; Miller, J. S.; Lafuente, P.; Novoa, J. J. *Chem.—Eur. J.* **2002**, *8*, 4894. (d) Jakowski, J.; Simons, J. *J. Am. Chem. Soc.* **2003**, *125*, 16089. (e) Jung, Y.; Head-Gordon, M. *Phys. Chem. Chem. Phys.* **2004**, *6*, 2008. (f) Scherlis, D. A.; Marzari, N. *J. Phys. Chem. B* **2004**, *108*, 17791. (g) Brocks, G. *J. Chem. Phys.* **2000**, *112*, 5353. (h) Devic, T.; Yuan, M.; Adams, J.; Fredrickson, D. C.; Lee, S.; Venkataraman, D. *J. Am. Chem. Soc.* **2005**, *127*, 14616.
(11) See, for example: (a) Ishiguro, T.; Yamaji, K.; Saito, G. *Organic Superconductors*, 2nd ed.; Springer: Berlin, 1998. (b) Williams, J. M.; Ferraro, J. R.; Thorn, R. J.; Carlson, K. D.; Geiser, U.; Wang, H. H.; Kini, A. M.; Whangbo, M.-H. *Organic Superconductors (Including Fullerenes): Synthesis, Structure, Properties, and Theory*; Prentice Hall: Englewood Cliffs, NJ, 1992.
(12) (a) Huang, J.; Kertesz, M. *J. Am. Chem. Soc.* **2006**, *128*, 1418. (b) Böhlin, J.; Hansson, A.; Stafström, S. *Phys. Rev. B: Condens. Matter Mater. Phys.* **2006**, *74*, 155111.
(13) Kubo, T.; Shimizu, A.; Sakamoto, M.; Uruichi, M.; Yakushi, K.; Nakano, M.; Shiomi, D.; Sato, K.; Takui, T.; Morita, Y.; Nakasuji, K. *Angew. Chem., Int. Ed.* **2005**, *44*, 6564. The crystal structure of **4** can be obtained from CCDC (deposition number 275077).
(14) Ohashi, K.; Kubo, T.; Masui, T.; Yamamoto, K.; Nakasuji, K.; Takui, T.; Kai, Y.; Murata, I. *J. Am. Chem. Soc.* **1998**, *120*, 2018.
(15) Nakasuji, K.; Kubo, T. *Bull. Chem. Soc. Jpn.* **2004**, *77*, 1791.
(16) The bulky *tert*-butyl groups in **3** do not allow a face-to-face $\pi-\pi$ intermolecular packing of the phenalenyl units, while this is possible for **1**. This is because the *tert*-butyl groups of **3** are attached to spin-bearing C atoms and they bump into each other when forming π-stacking, while the *tert*-butyl groups of the π-dimer of **1** are staggered. In the case of **2**, such a $\pi-\pi$ intermolecular packing of the phenalenyl units is possible.
(17) Transfer integral t is used interchangeably with resonance integral β.
(18) The term "alternating chain" does not mean the two resonance structures shown in Scheme 4 of ref 13, but means that the intermolecular and intramolecular interactions exist simultaneously, leading to two magnetic exchange parameters not equal to each other.

in the same way[13] as in the case of **3**,[14] in terms of the simple Bleaney−Bowers *dimer model*[19] for two coupled spins instead of using an alternating chain model for an infinite number of spins coupled by two alternating exchange parameters J_1 and J_2 (one for intramolecular coupling and the other for intermolecular coupling). The dimer model provided a large $J_1 = -2200$ K (−0.19 eV) and a zero J_2 for the chain of **2**.[13,20] This J_1 value from the Bleaney−Bowers fit seems to agree well with the J_1 value (−2460 K or −0.21 eV) of **3** obtained from ESR measurement, which is undoubtedly from intramolecular coupling in **3** where the dimer model is expected to be very accurate. However, the π-chain structure and the corresponding broad energy bands along the chain raise the issue whether an alternative interpretation with $J_2 \neq 0$ should be considered for **2** and that intermolecular covalent $\pi-\pi$ bonding may be playing an important role on the physical properties of **2**.

Our interest in this problem is motivated by the recent focus on the intermolecular multicenter covalent $\pi-\pi$ bonding interaction between neutral and charged organic radicals.[2−4,8−10,12] We hope to gain further insights into the intermolecular interactions coming from the $\pi-\pi$ overlap of SOMO electrons in the phenalenyl units by studying the effects of such $\pi-\pi$ bonding on geometrical and electronic structures and magnetic properties of these BPBR systems. We first present the geometry studies by ab initio calculations showing the effects of multicenter covalent $\pi-\pi$ bonding interaction on bond distances on the basis of the hypothesis that such intermolecular interactions are absent in **3** and are significant in the chains of **2**. We suggest that the SOMO electrons in the π-chains of **2** are participating in the intermolecular covalent $\pi-\pi$ bonding making them partially localized on the phenalenyl units and less available for intramolecular delocalization, leading to the observed geometrical changes. Further evidence on the partial localization of the SOMO electrons is obtained by studying the geometries of (di)cations and various related molecules of **2**. Then we address the band structure and obtain information on the transfer integrals, which are used to assist our new analysis of the experimental magnetism data using an alternating chain model for the π-chains of **2**. These studies from various perspectives provide unified evidence of multicenter covalent $\pi-\pi$ bonding interaction and its effects on molecular and solid-state properties.

Theoretical Considerations

We use the convention for magnetic exchange parameters, $J_{i,j}$ (i and j are neighbors), to define the Heisenberg Hamiltonian for a chain of $S = {}^1/_2$ spins

$$H = -\sum_{j>i} J_{i,j} S_i S_j \tag{1}$$

For antiferromagnetic coupling, $J_{i,j} < 0$. For an alternating chain, we assume two different kinds of first-neighbor exchange parameters, J_1 and J_2. This alternating chain is intermediate between two extremes. In the regular linear chain, $J_1 = J_2$. In the dimer case, one of the two J values is zero. As we shall see in the magnetism section, the alternating Heisenberg chain model is the correct model to describe the magnetic susceptibility of the molecular crystal **2**, providing us with two different exchange parameters J_1 and J_2. At this point, it is not a priori known which of the two exchange parameters corresponds to intra- and intermolecular interactions, respectively.

According to this convention, in the case of a dimer,[21]

$$\Delta E_{ST} = J \tag{2}$$

where

$$\Delta E_{ST} = E_{singlet} - E_{triplet} \tag{3}$$

Equation 3 will be used to calculate the singlet−triplet energy difference for isolated molecules of **2** and **3** which can be thought of as "dimers" owing to the presence of two phenalenyl units and two SOMO electrons. Note that the term "dimer" in this context is different from that in the dimer calculations of Kubo et al.[13] using two π-stacked molecules of **2**. Equation 2 will be used to bridge the gap between our ab initio "dimer" calculations on **2** and **3**, and the experimental magnetic data of **3**, and our alternating chain analysis of the magnetic susceptibilities of **2**.

In the band calculation section, we use the following simple band model to analyze the band structure of **2** obtained from ab initio calculations[22]

$$E(k) = \alpha \pm \sqrt{t_1^2 + t_2^2 + 2t_1 t_2 \cos(k)} \tag{4}$$

where t_1 and t_2 are two alternating transfer integrals associated with intra- and intermolecular SOMO−SOMO interactions, respectively, α is the Coulomb integral, and k is the wave vector. We shall see that eq 4 is adequate to describe the energy bands of **2** derived from the SOMO electrons.

Intuition may not be helpful to estimate the relative magnitudes of the intra- versus intermolecular coupling (J_1 vs J_2) of the SOMO electrons. The relationship between J and t is thus pivotal in helping to assign the two exchange parameters J_1 and J_2 to intra- and intermolecular interactions. Here we use the Hubbard model[23] with a transfer integral t and an on-site Coulomb repulsion energy, also called Hubbard U, which corresponds to the effective electron−electron repulsion of two electrons on one phenalenyl unit. The U value is on the order of 1 eV for π-radicals.[24] We will address the U values in connection with the analysis of the magnetism of the stepped π-chains of **2**. Within the Hubbard model, the exact solution of

(19) See, for example: Kahn, O. *Molecular Magnetism*; VCH Publishers: New York, 1993; pp 103−111.

(20) It is not a priori known which of the two exchange parameters corresponds to intra- and intermolecular interactions, respectively. The assignment of J_1 to intramolecular and J_2 to intermolecular interactions is based on transfer integrals associated with the intramolecular and intermolecular SOMO−SOMO overlaps. See the magnetism section.

(21) Kawakami, T. In *Molecular Magnetism-New Magnetic Materials*; Itoh, K., Kinoshita, M., Eds.; Kodansha Ltd., Gordon and Beach Science Publishers: Tokyo, Amsterdam, 2000; pp 9−10.

(22) See, for example: Kertesz, M. *Int. Rev. Phys. Chem.* **1985**, *4*, 125.

(23) (a) Harris, A. B.; Lange, R. V. *Phys. Rev.* **1967**, *157*, 295. (b) Rice, M. J. *Solid State Commun.* **1979**, *31*, 93. (c) Pincus, P. In *Selected Topics in Physics, Astrophysics, and Biophysics*; Abecassis de Laredo, E., Jurisic, N. K., Eds.; D. Reidel Publishing Co.: Dordrecht-Holland, The Netherlands, 1973; p 152. (d) Soos, Z. G.; Bondeson, S. R. In *Extended Linear Chain Compounds*; Miller, J. S., Ed.; Plenum Press: New York, 1983; Vol. 3, p 196.

(24) (a) Short-range electron correlation plays a significant role in determining the U value. See Ohno, K.; Noguchi, Y.; Yokoi, T.; Ishii, S.; Takeda, J.; Furuya, M. *ChemPhysChem* **2006**, *7*, 1820. The larger the SOMO electron delocalization domain, the smaller the U value because the two electrons have larger space to avoid each other. (b) For an example of U = ca. 1 eV for organic radicals with intermediate domains, see, for example: Tanner, D. B. In *Extended Linear Chain Compounds*; Miller, J. S., Ed.; Plenum Press: New York, 1983; Vol. 2, p 205. (c) For the U value of ca. 1 eV for the title compounds, see refs. 13 and 14.

singlet−triplet energy difference for a dimer is[23]

$$\Delta E_{ST} = U/2 - \sqrt{4t^2 + (U/2)^2} \quad (5)$$

which reduces in the limit of large t to the expression[25]

$$\Delta E_{ST} = J = -2|t| + U/2 \quad (6)$$

We will apply these relationships to the chains of **2** assuming that the chains consist of two kinds of "dimers", where the term "dimer" refers to a coupled pair of two phenalenyl sites. Therefore, one kind of "dimer" is molecule **2** itself, as noted before, and the other involves the π-stacked two phenalenyl units in the experimentally observed configuration of the chain of **2**. These are illustrated in Figure 1 as the horizontally and vertically oriented ellipses, respectively. Accordingly, there exist two kinds of t (t_1 and t_2) and J (J_1 and J_2) values along the chain of **2**. In the last section on magnetism, we shall use eq 6 to check the consistency of the various parameters (t, J, and U) obtained for **2** from ab initio dimer and band structure calculations, magnetic susceptibility analysis, and electrochemistry.

Computational Methodology

The full geometry optimizations of the BPBRs and relevant molecules were performed for the ground singlet states with the GAUSSIAN 03 program[26] by density-functional theory (DFT) using Becke's three-parameter hybrid density functional in combination with Lee−Yang−Parr correlation functional (B3LYP)[27] and the 6-31G* basis set. This model chemistry was validated on the basis of the geometry optimization results for **3**. According to our earlier basis set convergence study, we found that the double-ζ plus polarization basis set 6-31G* is appropriate to obtain sufficiently converged intermolecular transfer integrals for the $\pi-\pi$ overlap across the van der Waals gap for organic molecular materials containing first-row atoms.[28] Optimization for the unsubstituted BPBR with the larger basis set of 6-311+G(2d) gave virtually the same geometry as that with 6-31G*. Both the spin-restricted method (RB3LYP) and the broken-symmetry, spin-unrestricted method (UB3LYP) were employed. For the UB3LYP calculations, the HOMO and LUMO are mixed to lift the spatial symmetries, thus producing unrestricted wave functions for the initial guess of the singlet states. The geometry optimization of the single chain of **2** was performed with the RB3LYP method by using periodic boundary conditions in the GAUSSIAN 03 program with a set of 68 k-points. This optimization was constrained by keeping the intermolecular separations of the overlapping C−C pairs fixed at the observed X-ray structure.

The band structure was obtained from DFT solid-state calculations performed on the X-ray structure of molecule **2** without the solvent molecules using the Vienna ab initio simulation package (VASP).[29] On the basis of our earlier validation of the model chemistry for band dispersion calculations for organic conducting materials involving intermolecular $\pi-\pi$ stacks,[28,30] we used for the solid-state calculations a PW91 exchange-correlation functional[31] and a plane-wave basis set with a kinetic energy cutoff of 286.7 eV. The eigenvalues from the VASP calculations were shifted up by 0.601 eV so that the Fermi level is located at 0 eV. The k-mesh is set to $1 \times 20 \times 1$, with the band structure sampled along the **b*** direction, which is parallel to the direct space vector **b** and the quasi 1-D chain. Other directions have negligible band dispersions according to the extended Hückel theory (EHT) band calculations of Kubo et al.[13]

The magnetic susceptibility data of **2** measured by SQUID were scanned in from the supplementary Figure S6 of ref 13 and analyzed with an alternating Heisenberg chain model. Details are given in the magnetism section. To clarify the exchange parameters obtained from magnetic susceptibility analysis, we calculated the intramolecular ΔE_{ST} values on the basis of the total energy calculations for isolated molecules of **2** and **3**. Both singlet and triplet energies were calculated using the R(U)B3LYP optimized singlet geometries of **2** and **3** in addition to the X-ray structures of **2**. These total energy calculations were performed at the B3LYP/6-31G* level, which has been widely used for ΔE_{ST} calculations, giving good agreement with post-HF correlation calculations and with experiments for a variety of organic and inorganic molecules.[32]

Results and Discussion

The Geometries of the Molecules. The geometries of **2** and **3** can have several resonance contributions as shown in Scheme 2. The linking *s*-indacene fragment is an antiaromatic 12-π electron system for which the delocalized (as in **2** and **3**) and localized (as in **2′** and **3′** or in **2″** and **3″**) structures are close in energy.[33] It is expected that small external perturbations can change the interplay between the Kekulé structures (**2**, **3**) and the biradicaloid structures (**2′**, **3′** and **2″**, **3″**) of the BPBR molecules. These two BPBR molecules appear to have fundamentally the same molecular structure. However, the packing as determined by X-ray crystallography exhibits remarkable differences.[16] We assume that the molecular geometries of **2** and **3** are also different because of the different intermolecular interaction. Therefore, the geometry study can serve as an indirect indicator of the intermolecular $\pi-\pi$ bonding interactions.

Here we explore the effect of this $\pi-\pi$ bonding on the differences in the observed and calculated intramolecular bond distances between **2** and **3**. We performed geometry optimization for the ground singlet states of both **2** and **3**, and the corresponding data are presented in Tables 1 and 2. Due to the biradicaloid structures involved, we performed both RB3LYP and UB3LYP calculations, where the former gives results for closed-shell singlets and the latter for open-shell singlets.

In Table 1 are also included the geometries of the unsubstituted BPBR optimized with two different basis sets. The larger basis set of 6-311+G(2d) gives virtually the same geometry as that obtained with 6-31G*, with differences of bond distances smaller than 0.6 pm. Our experience with another similar molecule, cyclo-biphenalenyl, shows that optimization with the larger basis set of 6-311+G(2d) also gives virtually the same

(25) Whangbo, M.-H. *J. Chem. Phys.* **1979**, *70*, 4963.
(26) Frisch, M. J.; et al. *Gaussian 03*, revision B.04; Gaussian, Inc.: Pittsburgh, PA, 2003.
(27) (a) Becke, A. D. *J. Chem. Phys.* **1993**, *98*, 5648.(b) Lee, C.; Yang, W.; Parr, R. G. *Phys. Rev. B: Condens. Matter Mater. Phys.* **1988**, *37*, 785.
(28) Huang, J.; Kertesz, M. *Chem. Phys. Lett.* **2004**, *390*, 110.
(29) (a) Kresse, G.; Furthmüller, J. *Phys. Rev. B: Condens. Matter Mater. Phys.* **1996**, *54*, 11169. (b) Kresse, G.; Hafner, J. *Phys. Rev. B: Condens. Matter Mater. Phys.* **1993**, *47*, 558. (c) Using Vanderbilt-type (Vanderbilt, D. *Phys. Rev. B: Condens. Matter Mater. Phys.* **1990**, *41*, 7892) untrasoft pseudopotentials (Kresse, G.; Hafner, J. *J. Phys.: Condens. Matter* **1994**, *6*, 8245).
(30) Huang, J.; Kertesz, M. *J. Chem. Phys.* **2005**, *122*, 234707.
(31) Perdew, J. P.; Wang, Y. *Phys. Rev. B: Condens. Matter Mater. Phys.* **1992**, *45*, 13244.
(32) (a) Gogonea, V.; Schleyer, P. v. R.; Schreiner, P. R. *Angew. Chem., Int. Ed.* **1998**, *37*, 1945. (b) Ito, A.; Ino, H.; Ichiki, H.; Tanaka, K. *J. Phys. Chem. A* **2002**, *106*, 8716. (c) Ruiz, E.; Alemany, P.; Alvarez, S.; Cano, J. *J. Am. Chem. Soc.* **1997**, *119*, 1297. (d) Wittbrodt, J. M.; Schlegel, H. B. *J. Chem. Phys.* **1996**, *105*, 6574.
(33) (a) Dunitz, J. D.; Krüger, C.; Irngaringer, H.; Maverick, E. F.; Wang, Y.; Nixdorf, M.; *Angew. Chem., Int. Ed. Engl.* **1988**, *27*, 387. (b) Hertwig, R. H.; Holthausen, M. C.; Koch, W.; Maksic, Z. B. *Angew. Chem., Int. Ed. Engl.* **1994**, *33*, 1192. (c) Nendel, M.; Goldfuss, B.; Houk, K. N.; Hafner, H. *THEOCHEM* **1999**, *461−462*, 23. (d) Choi, C. H.; Kertesz, M.; Jiao, H.; Schleyer, P. v. R. Unpublished results, 2002−2004. See in Kertesz, M.; Choi, C. H.; Yang, S. *Chem. Rev.* **2005**, *105*, 3448.

Table 1. Optimized Bond Distances of Unsubstituted BPBR and the *tert*-Butyl-Substituted BPBR **3** Compared with Those of the X-ray Structure of **3**

	unsubstituted BPBR		**3**		
bond index[a]	RB3LYP (Å)[b]	RB3LYP (Å)[c]	RB3LYP (Å)[b]	UB3LYP (Å)[b]	X-ray (Å)[d]
a	1.446	1.443	1.446	1.455	1.450(4)
b	1.453	1.450	1.451	1.445	1.437(5)
c	1.396	1.392	1.396	1.396	1.394(3)
d	1.399	1.393	1.393	1.393	1.377(4)
e	1.409	1.404	1.411	1.414	1.411(4)
f	1.437	1.433	1.468	1.464	1.453(4)
g	1.387	1.381	1.393	1.398	1.391(4)
h	1.415	1.411	1.407	1.402	1.404(4)
i	1.425	1.421	1.440	1.441	1.433(3)
j	1.393	1.388	1.392	1.392	1.389(5)
k	1.417	1.413	1.410	1.409	1.399(4)
rms dev	0.0114	0.0109	0.0090	0.0083	
rms dev of bonds *a*, *b*, and *c*	0.0096	0.0086	0.0085	0.0056	

[a] See Scheme 2. [b] 6-31G* basis set. [c] 6-311+G(2d) basis set. [d] Reference 14.

geometry as that with 6-31G*.[4] For the rest geometry optimizations, we use the basis set of 6-31G*. These bond distances of the unsubstituted BPBR optimized with RB3LYP/6-31G* are very close to those of **3** optimized at the same level of theory, except for bonds *f* and *i*,[34] indicating that the substitution effect of the *tert*-butyl groups is small. With RB3LYP, the agreement for **3** between the calculation and the X-ray structure is within 1.6 pm for all bonds and less than 1 pm for most. There is a slight improvement when the theory is changed to UB3LYP, as can be seen from the slightly smaller root-mean-square (rms) deviation with UB3LYP. This reflects the biradical character of the molecule as indicated by the total spin expectation value of $<S^2> = 0.617$. However, the improvement of the geometry is very small, in correspondence with the finding that the singlet biradical character of the unsubstituted **3** is on the order of only 30%.[13] As indicated by Scheme 2, bonds *a*, *b*, and *c* may be particularly sensitive to whether the two SOMO radical electrons are delocalized through the bonds of *s*-indacene or partially localized on the two phenalenyl units. With UB3LYP, bond *a* is slightly longer than bond *b* by ca. 1 pm. This calculated difference is close to the experimentally observed difference. On the basis of the small rms deviations and the small biradical character, we conclude that both RB3LYP and UB3LYP should be satisfactory for geometry optimization for this system.

The agreement between the bond distances calculated at the same level of theory for **2** are not as good as for **3** as shown by columns 2 and 3 of Table 2 as compared with the experimental data in the last column. The problem is particular to bonds *a* and *b*, and to a lesser degree to bond *h*, otherwise the quality of the agreement between experiment and theory is similar to that of **3**. UB3LYP improves the agreement, but bonds *a* and *b* are comparable with RB3LYP and differ from each other only by ca. 1 pm with UB3LYP, while X-ray structure shows that bond *a* is longer than bond *b* by 4 pm. Where is this discrepancy coming from?

Aside from the calculations, the difference in the X-ray values of the bond distances of bonds *a* and *b* between **2** and **3** is noteworthy and significant. Our hypothesis is that this difference comes from the different intermolecular interactions associated with different packing in the crystals of **2** and **3.** Since **3** is isolated in the solid state as a result of bulky *tert*-butyl groups,[16] intermolecular covalent $\pi-\pi$ bonding is absent. The two SOMO radical electrons in **3** couple intramolecularly through bonds, pushing bond *b* toward a typical $C(sp^2)-C(sp^2)$ single bond distance of 1.46 Å.[35] Therefore, its structure is better described as the structure **3** instead of **3′** or **3″** in Scheme 2. In contrast, the SOMO electrons in **2** are participating in intermolecular covalent $\pi-\pi$ bonding making them less available for intramolecular delocalization, leading to partial localizations of the SOMO electrons on each phenalenyl unit, and the experimentally observed elongation of bond *a* by about 2 pm together with the shortening of bond *b* by 1 pm going from **3** to **2**. Therefore, its structure is better described as the structure **2″** in Scheme 2.

This argument about the role of the phenalenyl SOMO electrons in the geometrical differences observed between **2** and **3** can be buttressed by molecule **4** where the two phenalenyl units are replaced by closed-shell naphthalene units as shown in Chart 2. Molecule **4** has no biradicaloid character and therefore its intramolecular coupling of two SOMO electrons is absent compared to **2** and **3**. Bond *a* in this case is expected to be longer, as indicated by the VB structure shown in Chart 2. RB3LYP optimization gives bond distances of 1.478, 1.432, and 1.403 Å for bonds *a*, *b* and *c*, respectively, in excellent agreement with the X-ray structure where the three corresponding bond distances are 1.479(2), 1.421(3), and 1.398(2) Å.[36] The experimental data for **2**, **3**, and **4** show a trend that bond *a* lengthens and bond *b* shortens, while bond *c* is virtually unchanged in the series going from **3** to **2** and to **4**. On the basis of these experimental facts alone, one might conclude that the SOMO electrons become partially paired in the intermolecular $\pi-\pi$ bonding interaction in **2** leading to a structure that is intermediate between **3** and **4**. This trend also shows how the geometry of the benzene ring of the *s*-indacene linkage changes from a somewhat quinonoid-like structure to a benzoid-like structure going from **3** to **2** and to **4**. The structure of **4** may be considered as the limiting case, where the total absence of the SOMO electrons produces the longest bond *a* and the shortest bond *b* in the series. This shows that the intermolecular coupling effect is not negligible, which explains the significant difference of bonds *a* and *b* in the experimental structure for **2** and the discrepancy between the R(U)B3LYP and X-ray structures of **2**.

If we include the intermolecular interactions in the calculations by optimizing the geometry of the whole chain of **2**, we obtain an excellent agreement between experimental and calculated bond distance within **2**, as shown in column 4 of Table 2. This significant improvement should be ascribed to the intermolecular $\pi-\pi$ bonding interaction making the two SOMO electrons on π-stacked phenalenyl units coupled intermoleuclarly across the $\pi-\pi$ overlap and less available in the intramolecular coupling. To clarify this point, we introduce the hypothetical complex **5** shown in Chart 3 that contains one molecule of **2** supplemented by two phenalenyl radicals in a

(34) This may result from the substitution of *tert*-butyl groups since in the case of **2** all bond distances agree with those of the unsubstituted BPBR including bonds *f* and *i* (see Table 2).

(35) Pople, J. A.; Gordon, M. *J. Am. Chem. Soc.* **1967**, *89*, 4253.

(36) Watson, W. H.; Kashyap, R. P.; Plummer, B. F.; Reese, W. G. *Acta Crystallog., Sect. C: Cryst. Struct. Commun.* **1991**, *47*, 1848.

Table 2. Optimized Geometries of **2** Compared with Its X-ray Structure and a Complex **5**

	2			**5**[b,c]	X-ray structure of **2** (Å)[d]
	isolated molecule		1-D chain[e]		
bond index[a]	RB3LYP (Å)[f]	UB3LYP (Å)[f]	RB3LYP (Å)[f]	RB3LYP (Å)[f]	average
a	1.449	1.459	1.471	1.470	1.470
b	1.454	1.447	1.441	1.442	1.429
c	1.404	1.404	1.404	1.404	1.398
d	1.398	1.398	1.396	1.397	1.391
e	1.409	1.412	1.414	1.414	1.410
f	1.435	1.432	1.427	1.427	1.423
g	1.386	1.391	1.397	1.396	1.391
h	1.418	1.412	1.406	1.406	1.402
i	1.425	1.425	1.425	1.426	1.417
j	1.395	1.394	1.395	1.395	1.393
k	1.417	1.416	1.415	1.415	1.408
rms dev	0.0125	0.0088	0.0061	0.0064	
rms dev of bonds a,*b*,*c*	0.0192	0.0127	0.0078	0.0083	

[a] See Scheme 2. [b] The bond indexing of the biradical part in complex **5** follows that in Scheme 2. [c] The intermolecular separations of the overlapping C−C pairs are fixed to 3.137 Å. [d] Reference 13. [e] The intermolecular separations of the overlapping C−C pairs are fixed exactly as in the X-ray structure. [f] Basis set used is 6-31G*.

Chart 2. Molecular Structure of 7,14-Diphenylacenaphtho[1,2-*k*]fluoranthene (**4**)

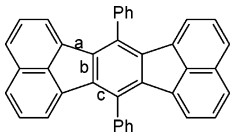

4

Chart 3. Top (a) and Side (b) Views of the Hypothetical Complex **5** Composed of Molecule **2** Coupled by Two Phenalenyl Radicals with One above (Thicker) and One below (Dashed)

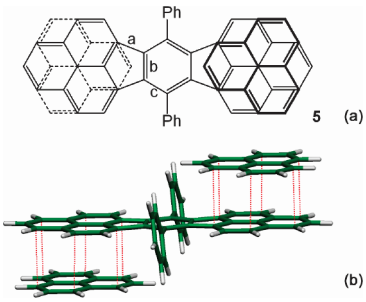

5

geometrical arrangement close to those observed in the π-dimer of **1** and the stepped chains of the crystal structure of **2**. This packing simulates the immediate neighbors of molecule **2** in its crystal structure and we view **5** as the smallest unit that contains all the essential interactions of the stepped π-chain. This model allows us to perform quantum chemical calculations at the RB3LYP/6-31G* level that proved to be sufficiently accurate for **3**. During the constrained geometry optimization the interplanar separation of the phenalenyls is kept at 3.137 Å, the same as the average interplanar separation in the X-ray structure of **2**. **5** contains four SOMO electrons corresponding to the four phenalenyl units, but it is formally a closed-shell system. The optimization of **5** was performed for singlet state for the following reasons. Similar to the π-dimer of **1**, the two SOMO electrons on the π-stacked phenalenyl units of **5** should couple antiferromagnetically through space via the intermolecular $\pi-\pi$ bonding interaction. The intramolecular coupling of two SOMO electrons within the biradical part of **5** should be similar to that of **3** being also antiferromagnetic. These antiferromagnetic couplings of SOMO electrons are corroborated by the fitting results of the magnetic susceptibility of **2** as shown in the magnetism section.

Table 3. Comparison of the Structures of Neutral **2** and Its Monocation and Dication

	2	$\mathbf{2}^{+}$	$\mathbf{2}^{2+}$	$\mathbf{2}^{2-}$	**2**
bond index[a]	RB3LYP (Å)[b]	UB3LYP (Å)[b]	RB3LYP (Å)[b]	RB3LYP (Å)[b]	X-ray (Å)[c]
a	1.449	1.469	1.487	1.457	1.470
b	1.454	1.437	1.425	1.459	1.429
c	1.404	1.404	1.405	1.408	1.398
rms dev	0.0192	0.0058	0.0109		

[a] See Scheme 2. [b] Basis set used is 6-31G*. [c] Chain structure.

The bond distances obtained for the BPBR part of complex **5** are shown in Table 2. They are almost identical to the 1-D chain calculations of **2** and prove that model **5** captures the essential interactions that influence the geometry of the 1-D chain of **2**. In both cases, especially significant is the elongation of bond *a* as well as the shortening of bond *b*, although the difference with the experimental value for the latter remains 1.3 pm. Bond *h* is also significantly improved. It appears that our hypothesis describes a good part of the discrepancy between the experimentally observed bond distances between **2** and **3** and can be taken as a strong indication that the intermolecular $\pi-\pi$ bonding interactions are sufficiently strong in the chains of molecule **2** that their effect influences intramolecular bond distances by 1−2 pm. The optimization of **5** without constraint gives an interplanar separation of 3.319 Å (averaged value over seven pairs of centers), which is close to that observed in the π-dimer of **1**,[8] still showing some intermolecular covalent bonding effect. With this larger separation than the constrained 3.137 Å separation, one can expect that the effect of intermolecular coupling on molecular geometry is smaller. As a result, the agreement between RB3LYP optimized bond distances of **5** with the X-ray structure of **2** is slightly worse, with an rms deviation of 0.0070 for bonds *a*−*k* and 0.0094 for bonds *a*−*c*.[37] We can also see from this discussion that it is challenging to obtain accurate interplanar separation, which requires very high order theory, for example, counterpoise-corrected MP2 calculations.[2]

The effect of the intermolecular $\pi-\pi$ bonding on the intramolecular bond distances can be further traced by comparing the optimized geometries of **2** and its monocation and dication. We used RB3LYP/6-31G* for closed-shell dication and UB3LYP/6-31G* for open-shell cation. This model chemistry has not been validated for charged species although it has been shown to be sufficient for the neutral BPBR systems. The point is to qualitatively analyze the trend shown in the bond distances which may provide us with insight into the number of electrons available in the HOMO and the location of the SOMO electrons.[7c] Key bonds are compared in Table 3. The changes of the bond distances can be interpreted by the use of the two frontier orbitals (Figure 2), which are combinations of the SOMOs on the phenalenyl units and the *s*-indacene bridging unit. The HOMO has bonding characteristics for bond *a* and antibonding characteristics for bond *b* leading to a gradual

(37) Fully optimized bond distances of *a* through *k* for complex **5** are (in Å): 1.468, 1.444, 1.404, 1.397, 1.414, 1.428, 1.396, 1.407, 1.426, 1.395, and 1.416.

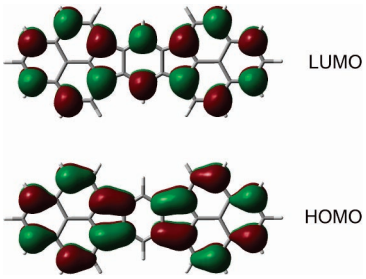

Figure 2. HOMO and LUMO of the molecule with the two phenyl groups of **2** replaced by hydrogen atoms. Calculated by RB3LYP/6-31G*.

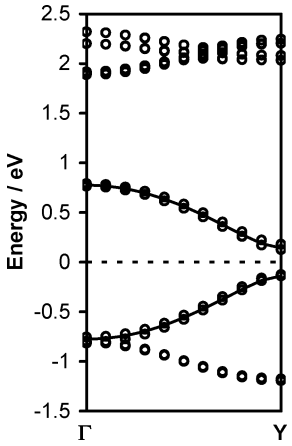

Figure 3. Band structure sampled along the chain direction of **2** (**b** // **b***) from the Γ point at $k = (0, 0, 0)$ to the Y point at $k = (0, \pi/|\mathbf{b}|, 0)$ in the Brillouin zone calculated with the PW91 density functional using the VASP program. The Fermi level (E_F) is indicated by the dashed line. The solid curves are the tight-binding fits using eq 4 discussed in the text.

increase and decrease of their respective lengths as the electrons are removed one by one. Table 3 shows this trend, while bond *c* does not change much being nonbonding for the HOMO. We present the dianion only for completeness. In that case, bonds *a*, *b*, and *c* are nonbonding and they change little relative to the neutral case.

These data provide further evidence for our hypothesis about the role of the covalent $\pi-\pi$ bonding played by the SOMO electrons in **2**. The critical bonds *a*, *b*, and *c* of $\mathbf{2}^+$ and $\mathbf{2}^{2+}$ agree better with the experimental geometry of **2** than the optimized geometry of **2** itself, further indicating that the SOMO electrons on the phenalenyl units of **2** are less available in the HOMO delocalization being partially participating in intermolecular through-space $\pi-\pi$ bonding. As we can see from the rms deviation, the net effect of the intermolecular $\pi-\pi$ bonding interaction seems to be that only about one of the two SOMO electrons is available for the intramolecular through-bond interactions in the *s*-indacene region of the molecule. Having established that there is significant intermolecular interaction in the case of **2**, now we move on to the electronic band structure to analyze the transfer integrals.

Band Calculations for BPBR Crystal 2. Figure 3 shows the energy band structure of **2** along **b*** in the reciprocal space for the bands close to the Fermi level, E_F. This is in fact along the chain direction in the direct space (**b** // **b***). The band structure displays quasi-degenerate pairs of bands. Each band exhibits an additional degeneracy that is not visible, so there are effectively four quasi-degenerate levels at each *k* point in the band structure owing to the fact that there are four molecules in the crystallographic unit cell ($Z = 4$).

The main dispersion occurs along the direction (**b**) of the stepped chains,[13] showing a very anisotropic band structure, in accordance with the highly anisotropic nature of the packing in the molecular crystal of **2**. Neighboring chains are only slightly coupled; the small splitting among the quasi-degenerate bands on the order of 50 meV is indicative of the very small dispersion in the perpendicular direction, which is therefore not reproduced here.

We focus here on the bands right below and above the Fermi level. The largest bandwidth *W* is found for the bands originating from the SOMO orbitals between 0.78 and −0.78 eV, giving a total *W* of 1.56 eV. This *W* value should be compared with that of the well-conducting cyclohexyl substituted SBP neutral radical crystal which also forms a quasi 1-D chain.[5,12] The corresponding *W* of cyclohexyl-SBP was found to be comparable (although only 1.1 eV) using the same model chemistry.[12] The value of $D = 3.28$ Å in the cyclohexyl-SBP chain is also comparable to the stepped chain of **2**, which is a bit shorter at $D = 3.137$ Å. On the other hand, there are significant differences between these two systems; most importantly, in the case of cyclohexyl-SBP, the bands are quarter filled (one SOMO electron per molecule), while here they are half filled in **2** (two SOMO electrons per molecule). This difference of band filling allows the metallic property for cyclohexyl-SBP and in the case of **2** results in a nonzero band gap making it into a semiconductor. However, in both phenalenyl-based materials, the good $\pi-\pi$ overlap of the phenalenyls produces an efficient pathway of intermolecular delocalization, not only within molecules, but also across the $\pi-\pi$ overlap between molecules.

The calculated total *W* of approximately 1.56 eV including the band gap shows significant electron delocalization, corresponding to an average effective transfer integral of $\bar{t} \approx 1.56/4 = 0.39$ eV. Of course, this value is an order of magnitude less than in conjugated polymers, such as polyacetylene, where the total π-electron bandwidth is about 10 eV.[38] Nevertheless, the *W* of 1.56 eV allows effective intermolecular $\pi-\pi$ overlap and electron delocalization which is a prerequisite for the through-space covalent $\pi-\pi$ bonding interactions between the SOMO electrons.

If we denote by t_1 and t_2 the intramolecular and intermolecular effective SOMO−SOMO interactions, and assume an infinite chain where these two values alternate, we arrive at an electronic structure that is fully analogous with the tight-binding electronic structure of polyacetylene where t_1 and t_2 take the roles of the two different Hückel resonance integrals.[22] We can fit the two SOMO-derived bands with eq 4 by setting α to the Fermi level at 0 eV. From this fit we obtain for the two transfer integrals $t_1 = 0.319$ eV and $t_2 = 0.460$ eV,[39] without being able to assign which of the two is the intra- or intermolecular value. [Incidentally, the corresponding average *t* values obtained by EHT[13] are similar, except that their difference, and therefore the corresponding gap, is much smaller.] The ratio of $t_1/t_2 =$

(38) See for example: Whangbo, M.-H.; Hoffmann, R.; Woodward, R. B. *Proc. R. Soc. London, Ser. A* **1979**, *366*, 23.

(39) (a) The tight-binding fit using the SigmaPlot program for the occupied bands gives $t_1 = 0.326$ eV and $t_2 = 0.455$ eV with an $R^2 = 0.9926$; the fit for the unoccupied bands gives $t_1 = 0.311$ eV and $t_2 = 0.465$ eV with an $R^2 = 0.9914$. (b) Instead of a fit, a simple calculation can be done using $E_g = 2|t_1 - t_2| = 0.28$ eV and $W = 2|t_1 + t_2| = 1.56$ eV coming from eq 4, giving $t_1 = 0.32$ eV and $t_2 = 0.46$ eV.

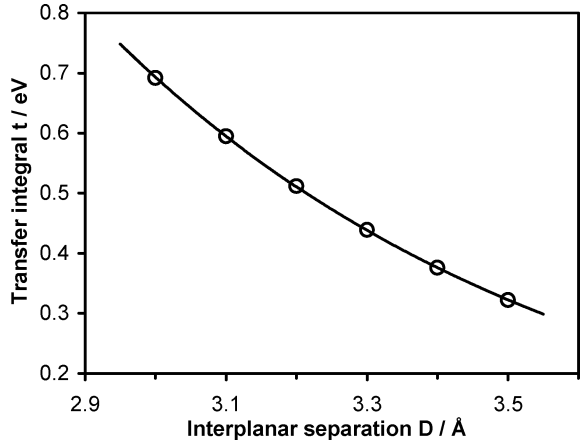

Figure 4. Transfer integrals t for the staggered phenalenyl π-dimers (geometry described in text) as a function of interplanar separation D calculated with PW91/6-31G*.

0.319/0.460 = 0.693 reflects the relative strength of the interactions, showing that the chain is not dimerized. We will return to this ratio when discussing the magnetism of **2** and **3**.

The band structure alone does not inform about whether the smaller or the larger value of t_1 or t_2 corresponds to the intra- or intermolecular coupling in the stepped chains of **2**. However, the phases of the crystal orbitals at the $k = \pi/|\mathbf{b}|$ point in the Brillouin zone clearly show that lower energy band has in-phase *inter*molecular interactions and out-of-phase *intra*molecular ones. For the higher energy level at the $k = \pi/|\mathbf{b}|$ point, the phases are the opposite. Thus, we can assign the smaller t_1 to the *intra*molecular interaction and the larger t_2 to the *inter*molecular interaction without ambiguity.

To corroborate the transfer integrals obtained from our band calculations, transfer integrals are calculated for the staggered phenalenyl π-dimers similar to **1** shown in Scheme 1 but with the *tert*-butyl groups replaced by hydrogens. Single-point calculations were performed with the GAUSSIAN 03 program using the PW91 exchange-correlation functional in combination with the 6-31G* basis set. (One can calculate intermolecular transfer integrals quite reliably with nonhybrid DFT using either sufficiently large Gaussian basis sets or plane wave basis sets.[28,30]) The C−C and C−H bond distances in each phenalenyl are fixed at 1.40 and 1.08 Å, respectively.[3] All bond angles are fixed at 120°, and each phenalenyl is completely planar. Interplanar separation D is in the range of 3.0−3.5 Å.

Figure 4 shows such calculated intermolecular $\pi-\pi$ transfer integrals as a function of D for the staggered phenalenyl π-dimer. The dependence of the transfer integrals on D is generally found to be close to exponential in the D = 2.7 to 3.5 Å region.[30,40] The intermolecular transfer integral value t_2 obtained from the band calculation for the chain of **2** at 0.46 eV is only ∼20% less than the value in Figure 4 for the observed D = 3.137 Å. This small difference is attributed to normalization and to the fact that the orbitals in **2** contain a small contribution from the *s*-indacene bridging unit as well. We conclude that the analysis of the band structure of the stepped chains of **2** indicates larger SOMO−SOMO transfer integrals between the molecules than within. Next we turn to magnetic exchange parameters of **2** and **3**.

Molecular Exchange Parameter Calculations. The magnetic susceptibilities of the molecular crystals **2** and **3** have been determined experimentally by solid-state ESR for **3**[14] and by solid-state SQUID for **2**.[13] The analysis of experimental measurements using SQUID is based on the Bleaney−Bowers equation[19] together with a consideration for the paramagnetic contributions from impurity P[41] often following Curie−Weiss law at low temperature:[42]

$$\chi_p(T) = \frac{2N_A g^2\beta^2}{k_B T[3 + \exp(-J/k_B T)]}(1 - P/2) + \frac{N_A g^2\beta^2}{4k_B(T-\theta)}P \quad (7)$$

where χ_p is the paramagnetic susceptibility, T is the temperature, N_A is Avogadro's number, g is the gyromagnetic factor, β is the electronic Bohr magneton, k_B is the Boltzmann constant, and θ is the Weiss temperature.[42b] P and J are obtained by fitting with the experimentally obtained susceptibility after the correction for diamagnetic contributions. This is often termed as the dimer model, but we should note that in this case the "dimer" is a virtual one consisting of the two SOMO electrons of a single molecule. The analysis of experimental data from ESR measurements uses an equation similar to eq 7 but the $\chi_p(T)$ is replaced by the integrated intensity of the ESR spectrum.[43]

Table 4. Comparison of Experimental J Values for the Crystals of **3** and **2** with Theoretical ΔE_{ST} from Isolated Molecule Calculations

	theoretical ΔE_{ST} (eV)			
	RB3LYP[a]	UB3LYP[a]	X-ray structure[b]	exptl J (eV)
3	−0.216	−0.248	NA	−0.212[c]
2	(−0.227)[d]	(−0.243)[d]	−0.204	−0.190[e]

[a] Optimizations were performed for singlet at the level of theory indicated, and the obtained geometries were used for triplet single point calculation; 6-31G* basis set. [b] The coordinates of the X-ray structure of **3** are not available (NA); the X-ray structure of **2** is used for singlet point UB3LYP calculations for singlet and triplet. [c] Solid-state ESR (ref 14). [d] Values in parenthesis are based on the optimized geometries, as listed in Table 2, which differ from the experiment as discussed in connection with Table 2. [e] Solid-state SQUID (ref 13).

Table 4 contains our theoretical ΔE_{ST} values and experimental intramolecular exchange parameters J for **2** and **3** obtained with the above dimer model. Both experiments on **2** and **3** indicate similar antiferromagnetic interactions. Here we discuss the possible interpretation of these experimental results using dimer calculations even though we have argued above that the significant intermolecular interactions in **2** should make it quite different from **3**. According to eqs 2 and 3, J is equal to ΔE_{ST}. This relationship allows us to compare the theoretical and experimental results in Table 4. Given the large uncertainties related to the experimental data in a relatively limited temperature range on one hand and various approximations in the theoretical calculations on the other hand, the first impression of these data might be that they all agree with one another quite well.

(40) (a) Senthikumar, K.; Grozema, F. C.; Bickelhaupt, F. M.; Siebbeles, L. D. A. *J. Chem. Phys.* **2003**, *119*, 9809. (b) Brédas, J. L.; Calbert, J. P.; da Silva Filho, D. A.; Cornil, J.; *Proc. Natl. Acad. Sci. U.S.A.* **2002**, *99*, 5804.
(41) P is on a per mol of BPBR molecule basis with two spins for each molecule.
(42) (a) For using Curie-Weiss law for impurities, see for example: Belik, A. A.; Azuma, M.; Takano, M. *Inorg. Chem.* **2005**, *44*, 7523. (b) Curie law can be used instead, where θ is approximated to be 0 if the residual $\chi(T)T$ coming from the paramagnetic impurity remains constant at low temperature.
(43) (a) Bleaney, B.; Bowers, K. D. *Proc. R. Soc. London, Ser. A* **1952**, 214. (b) Bijl, D.; Kainer, H.; Rose-Innes, A. C. *J. Chem. Phys.* **1959**, *30*, 765.

The agreement between the calculated ΔE_{ST} value by both RB3LYP and UB3LYP with the experimental J value of **3** is quite good. There is no reason to doubt the validity of the dimer model for compound **3** and its theoretical interpretation that results from the rather good agreement between calculation and experiment: **3** is a singlet ground state molecule with a low-lying triplet having some, albeit small, degree of biradicaloid character. The validity of the dimer model is justified by the packing motif of **3** where molecules are isolated and so the intermolecular coupling of SOMO electrons are negligible. The data in columns 2 and 3 in Table 4 indicate that the intramolecular ΔE_{ST} values of **2** and **3** should be very similar, given the similarity of these two molecular structures. Even though the experimental J seems to agree quite well with the ΔE_{ST} value calculated from the X-ray structure of **2** and with the ΔE_{ST} and J values of **3**, the dimer model is not applicable to **2** owing to the significant intermolecular coupling for the crystals of **2**.

Alternating Chain Model Fit of Magnetism for 2. On the basis of geometry and band structure studies and dimer calculations, here we investigate the possibility of interpreting the magnetism of **2** using an infinite alternating chain of $S = {}^1/_2$ spins as implied by the full Hamiltonian in eq 1. For weakly coupled alternating chains where the J values are small, the widely used Duffy−Barr−Hatfield equation[19,44] is sufficient to fit $\chi(T)T$; however, for strongly coupled alternating chains, the Duffy−Barr−Hatfield equation is not valid at low temperature.[44] Johnston et al.[45] have reviewed the rather extensive literature on nearly exact numerical calculations of such models and arrived at a very accurate fit for the susceptibility of such a Heisenberg chain expressed in terms of the larger one of the two J values and their ratio (the alternation parameter), $\alpha = J_1/J_2$, in the range of $0 \le \alpha \le 1$. We proceeded to use eq 56 in ref 45 to fit the temperature-dependent magnetic susceptibility data[46] in the 26−298 K range scanned in from the supplementary Figure S6 of ref 13. The $P = 1.64\%$ impurities as given in the analysis of Kubo et al.[13] are treated in the same way as in eq 7, and the Weiss temperature is approximated to be 0. The fit provides pairs of J and α values (shown in Figure 5) that differ only slightly in their overall rms deviation values.

The shape of the α-J curve indicates that the larger J value dominates the magnetic susceptibility. The rms deviation at $\alpha = 0$ is 0.0375, and the corresponding best fit is $J = -2200$ K $= -0.19$ eV, which is the same value as that from the Bleaney−Bowers fit. The increase of α and thus the smaller J value from 0 to about 40−50% has a small influence on the larger J value. These results show that although the Bleaney−Bowers fit ($\alpha = 0$) gives a quite good result, other fits are equally good, or slightly better. The rms deviation decreases somewhat to 0.0369 as α is increased to 0.3 and remains almost constant until $\alpha = 0.85$, beyond which it increases rapidly. The optimal fit is at about $J_2 = -4000$ K $= -0.34$ eV and $\alpha = 0.77$ (leading to $J_1 = -0.26$ eV) with an rms deviation of 0.0366. However, there is a range of parameters with essentially the same quality of fit, including $J_2 = -3340$ K $= -0.29$ eV and $\alpha = 0.68$ (leading to $J_1 = -0.20$ eV). Given the limited temperature range and the large spread of the original susceptibility data, the fit remains ambiguous. Nevertheless, it is important to observe that the best fit corresponds to an alternating Heisenberg chain, not to the dimer model. A reasonable choice appears to be: $J_2 = -0.29$ eV (intermolecular) and $J_1 = -0.20$ eV (intramolecular), with the latter agreeing well with the intramolecular J_1 values in Table 4. The fit corresponding to these parameters is compared to the Bleaney−Bowers fit and the experimental SQUID data points from ref 13 in Figure 6.

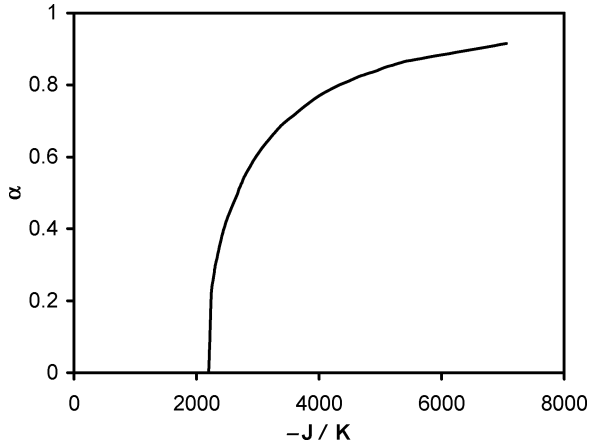

Figure 5. Pairs of J and α values obtained for the stepped chain of **2** by fitting the experimental $\chi_p(T)T$ values scanned in from Figure S6 of ref 13 with an alternating Heisenberg model based on eq 56 of ref 45.

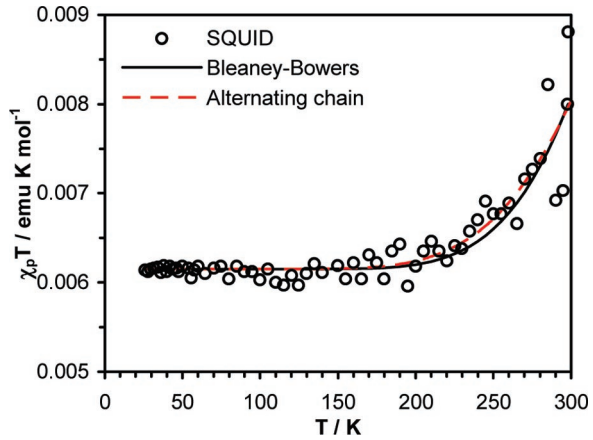

Figure 6. Comparison between an alternating Heisenberg chain fit (with $J = -3340$ K and $\alpha = 0.68$) and a Bleaney−Bowers fit (with $J = -2200$ K and $\alpha = 0$) on the $\chi_p(T)T$ data scanned in from the supplementary Figure S6 of ref 13 (SQUID measurements).

We are able to assign the smaller J value to the intramolecular exchange interaction and the larger one to the intermolecular $\pi-\pi$ interaction with the following reasoning. The exchange parameter of the monomeric system **3** has been very accurately described by the dimer model. The DFT calculations agree with that exchange parameter accurately, which is in the -0.21 to -0.25 eV range (Table 4). It is reasonable to assume that the intramolecular value in **2** would not substantially deviate from this range. In addition, the intermolecular $\pi-\pi$ exchange interaction has been determined in other phenalenyl-based dimer systems. For the staggered π-dimer **1** with an interplanar distance of $D = 3.2-3.3$ Å, Bleaney−Bowers fit of the ESR intensities provided -0.288 eV,[47] which is on the same order of magnitude as the estimate of $J_2 = -0.29$ eV from our

(44) (a) Duffy, W.; Barr, K. P. *Phys. Rev.* **1968**, *165*, 647. (b) Hall, J. W.; Marsh, W. E.; Weller, R. R.; Hatfield, W. E. *Inorg. Chem.* **1981**, *20*, 1033. (c) Hatfield, W. E. *J. Appl. Phys.* **1981**, *52*, 1985.
(45) Johnston, D. C.; Kremer, R. K.; Troyer, M.; Wang, X.; Klümper, A.; Bud'ko, S. L.; Panchula, A. F.; Canfield, P. C. *Phys. Rev. B: Condens. Matter Mater. Phys.* **2000**, *61*, 9558.
(46) Johnston, D. C. Private communication, 2006.

alternating chain fit for **2**. The third reason is straightforward from eq 6: the larger t is, the more negative J is, assuming ~1 eV for the Hubbard U.[24]

Now that we have obtained t from band-structure calculations and J from magnetic susceptibility analysis and molecular quantum chemical calculations, finally we can check whether various parameters obtained for **2** are consistent with one another. According to eq 6, the Hubbard on-site Coulomb repulsion U is related to J and t by

$$U = 2J + 4|t| \tag{8}$$

Reasonable estimates of U can be obtained from electrochemistry.[7,48] The disproportionation potential[7] for phenalenyl radical is 1.6 V,[49] leading to the estimate of $U = 1.6$ eV for phenalenyl. The U value of **1** is ca. 1.5 eV.[8a] Derivatives of phenalenyl tend to have smaller U values[50] because of the increased domain available for delocalization of the electrons and accordingly their reduced electron−electron repulsion in their anions relative to that of phenalenyl. The electrochemistry-based estimate for the Hubbard U yields approximately 1.1 eV for **2**[13] and 1.16 eV for **3**.[14] On the other hand, if we substitute $t_1 = 0.319$ eV and $J_1 = -0.20$ eV into eq 8, we obtain $U = 0.88$ eV; with $t_2 = 0.460$ eV and $J_2 = -0.29$ eV, we obtain $U = 1.26$ eV. These on-site Coulomb repulsion energies obtained from eq 8 are in good agreement with those of the BPBR molecules obtained from cyclic voltammetry, which is about 1.1 eV.[13,14]

Conclusions

In this paper, we have focused on the effects of intermolecular covalent $\pi-\pi$ bonding interaction on the molecular and crystal geometries, the electronic band structure, and magnetic susceptibility data for the molecular semiconductor of the biradicaloid molecule **2**, which forms a stepped π-chain showing good intermolecular $\pi-\pi$ overlap between π-stacked phenalenyl units, in sharp contrast to the X-ray structure of **3**. Ab initio calculations for the isolated molecular structure of **2** provide a different geometry from the crystal structure of **2**, whereas the agreement between theoretical and experimental structures for **3** is excellent. However, inclusion of intermolecular $\pi-\pi$ overlap in the geometry optimization by using the stepped π-chain of **2** and the hypothetical complex **5** results in significant changes of the geometry for **2**, yielding good agreement with experiments. These geometrical differences between **2** and **3** are attributed to the presence and absence of intermolecular $\pi-\pi$ bonding interaction for **2** and **3**, respectively, as implied by their different crystal packing motifs. The two SOMO electrons of the two phenalenyl units on the isolated molecule **3** couple through bonds and are therefore delocalized in the *s*-indacene bridging unit, while the two SOMO electrons on **2** are partially localized on the two phenalenyl units as they are participating in the through-space covalent $\pi-\pi$ bonding with π-stacked phenalenyl units on neighboring molecules. Analysis of the band structure provides two transfer integrals, $t_1 = 0.319$ eV and $t_2 = 0.460$ eV, corresponding to a weaker intramolecular through-bond SOMO−SOMO interaction and a stronger intermolecular through-space interaction. The relatively large bandwidth W and small band gap are consistent with the existence of intermolecular $\pi-\pi$ bonding interaction and semiconducting behavior. On the basis of these geometrical and electronic structure studies, we have presented an alternative interpretation for the magnetism of the stepped π-chain of **2** using an alternating Heisenberg chain model, giving two exchange parameters, $J_1 = -0.20$ eV and $J_2 = -0.29$ eV, corresponding to intra- and intermolecular interactions, respectively. The new interpretation of magnetism is consistent with ab initio total energy calculations for **2** and prevails against the previous interpretation using the Bleaney−Bowers dimer model which is naturally applicable to **3** but not to **2**. The transfer integrals and exchange parameters thus obtained fit well into the framework of the Hubbard model, leading to an on-site Coulomb−Hubbard U value of ca. 1 eV in good agreement with the experimental value from cyclic voltammetry. Given the limited temperature range and the large spread of the original magnetic susceptibility data, the presented alternating chain fit for the magnetic susceptibility of **2** remains ambiguous judging from the rms deviation. Nevertheless, all of the ab initio calculations, band structure analysis, and magnetic susceptibility calculations, when put together, allow us to provide a coherent picture for the alternating chain for **2** with significant intermolecular through-space covalent $\pi-\pi$ bonding interaction in its molecular crystal. Such understanding of the coexistence of intramolecular delocalization and intermolecular $\pi-\pi$ bonding interaction should be applicable to the understanding of the π-stacking in the earlier heterocyclic biradical[51] and the recent phenalenyl-based neutral radical conductor.[5,12]

Acknowledgment. Financial support from the National Science Foundation (Grant No. DMR-0331710) is gratefully acknowledged. We are indebted to Prof. Paul M. Lahti for his comments on broken-symmetry calculations and on fitting magnetic susceptibility data. We thank Prof. David C. Johnston for providing us with his computer code[46] for eq 56 of ref 45, which we used to write our fitting program for the magnetic susceptibility of infinite alternating chain of $S = {}^1/_2$ spins.

Supporting Information Available: Complete author list of ref 26, optimized geometries of the 1-D π-chain, isolated molecule, (di)cation, and dianion of **2**, optimized geometries of isolated **3**, **4**, and complex **5**, optimized geometry of BPBR without substitution, total energies of all calculated structures, and electron density isosurfaces of the Kohn−Sham crystal orbitals at the zone edges ($k = 0$ and $\pi/|\mathbf{b}|$) for the two bands closest to the Fermi level. This material is available free of charge via the Internet at http://pubs.acs.org.

JA066426G

(47) (a) Morita, Y.; Aoki, T.; Fukui, K.; Nakazawa, S.; Tamaki, K.; Suzuki, S.; Fuyuhiro, A.; Yamamoto, K.; Sato, K.; Shiomi, D.; Naito, A.; Takui, T.; Nakasuji, K. *Angew. Chem., Int. Ed.* **2002**, *41*, 1793. (b) Earlier SQUID measurement of **1** provided a rather low value of −0.17 eV (ref 8b).
(48) (a) Garito, A. F.; Heeger, A. J. *Acc. Chem. Res.* **1974**, *7*, 232. (b) Torrance, J. B. *Acc. Chem. Res.* **1979**, *12*, 79.
(49) Haddon, R. C.; Wudl, F.; Kaplan, M. L.; Marshall, J. H.; Cais, R. E.; Bramwell, F. B. *J. Am. Chem. Soc.* **1978**, *100*, 7629.
(50) (a) Koutentis, P. A.; Chen, Y.; Cao, Y.; Best, T. P.; Itkis, M. E.; Beer, L.; Oakley, R. T.; Cordes, A. W.; Brock, C. P.; Haddon, R. C. *J. Am. Chem. Soc.* **2001**, *123*, 3864. (b) Zheng, S.; Thompson, J. D.; Tontcheva, A.; Khan, S. I.; Rubin, Y. *Org. Lett.* **2005**, *7*, 1861.
(51) Banister, A. J.; Rawson, J. M.; Clegg, W.; Birkby, S. L. *J. Chem. Soc., Dalton Trans.* **1991**, 1099.